

Poly[methyl methacrylate (M)-*b*-styrene (S)-*b*-Butadiene (B)-*b*-S-*b*-M] Pentablock Copolymers: Synthesis, Morphology, and Properties

J. M. Yu,[†] Ph. Dubois, and R. Jérôme*

University of Liège, Center for Education and Research on Macromolecules, Sart-Tilman, B6, 4000 Liège, Belgium

Received December 19, 1996; Revised Manuscript Received May 23, 1997[®]

ABSTRACT: A series of poly[methyl methacrylate (M)-*b*-styrene (S)-*b*-butadiene (B)-*b*-S-*b*-M], or MSBSM, pentablock copolymers have been successfully synthesized by sequential living anionic polymerization initiated with the diadduct of *tert*-butyllithium (*t*-BuLi) onto *m*-diisopropenylbenzene (*m*-DIB) in a cyclohexane/diethyl ether mixture for the butadiene and styrene polymerization at room temperature and in a cyclohexane/THF mixture for the MMA polymerization at -78°C . All the pentablock copolymers have a monomodal and narrow molecular weight distribution ($M_w/M_n < 1.20$), and their weight composition varies from 11 to 55% M, 18 to 55% S, and 15 to 64% B. Toluene-cast films of these copolymers have been analyzed by differential scanning calorimetry (DSC), dynamic mechanical analysis (DMA), and transmission electron microscopy (TEM). All these materials show a phase separation of the soft B component from the hard S and M blocks, which cannot, however, be distinguished one from each other by DSC or DMA. Indeed, a single transition is observed for the binary hard phase at a temperature intermediate between the glass transition temperature of polystyrene (PS) and poly(methyl methacrylate) (PMMA). In addition to classical phase morphologies, such as cylindrical and lamellar phase organization, two nonclassical morphologies, i.e., catenoid–lamellar and strut phase structures have been observed by TEM. The phase morphology strongly depends on the pentablock composition and any chemical modification of blocks. For instance, the cylindrical morphology, characteristic of an MSBSM copolymer containing equal amounts of hard and soft phases, is changed into a lamellar morphology upon hydrogenation of the B midblock. Copolymers of a relatively low hard phase content typically behave as thermoplastic elastomers of high ultimate tensile strength (ca. 30 MPa) and elongation at break (ca. 900%). These mechanical properties, however, depend on the casting solvent.

Introduction

Styrene-*b*-butadiene-*b*-styrene (SBS) copolymers with a major content of B are well-known thermoplastic elastomers (TPE) that combine the mechanical properties of vulcanized rubbers and preserve the unique opportunity of thermoplastics of being easily processed. These unique thermomechanical properties are the direct consequence of the phase separation of minor polystyrene (PS) domains dispersed in a continuous rubbery polybutadiene (PBD) phase. The PS hard phase ($T_g = 100^{\circ}\text{C}$) plays the key role of physical crosslinks, which start, however, to be deformed and to creep even for low applied stresses as the glass transition temperature is approached. Accordingly, the practical usefulness of SBS is restricted to an upper temperature dictated by T_g of the outer blocks. Furthermore, the PS hard phase is poorly resistant to hydrocarbons and oils, which is an additional limitation to practical applications. It is thus a valuable target to increase this upper service temperature so as to approach that of vulcanized rubbers. As examples of strategies reported for this purpose, the PS outer blocks have been chemically modified^{1,2} and substituted by polymers of higher T_g .^{3–9} Very recently, as an alternative method, we have reported on the attachment of a syndiotactic poly(methyl methacrylate) (sPMMA) block at both ends of SBS, resulting in MSBSM pentablocks¹⁰ and in a significant increase of the upper service temperature of the original

triblock copolymers. The phase morphology of these new materials was, however, not discussed in this paper, although the mechanical performances of multiphase materials are known to be closely related to that characteristic feature.

Extensive studies of phase morphology have been reported for binary block systems of the AB and ABA type^{11–17} and for ternary copolymers of the ABC^{18–24} and ABACA^{25,26} type. In addition to classical spherical, cylindrical, and lamellar phase structures,³³ some nonclassical morphologies, such as ordered bicontinuous double-diamond (OBDD),¹³ and catenoid–lamellar,^{14,16,34} have been observed depending on block copolymer composition and sample preparation. Systematic morphological studies on symmetrical pentablock copolymers of the ABCBA type with sPMMA as the outer block and a soft PBD midblock have never been reported, at least to our best knowledge. Actually, the synthesis of this type of block copolymer was a challenge for a long time because of problems of monomer (MMA) purification and sensitivity of the carbonyl group of MMA toward nucleophilic attack.^{27,28} Furthermore, PMMA anions are unable to initiate the polymerization of dienes, which requires the availability of a difunctional initiator soluble in apolar solvents for the diene polymerization into living polydianions with the desired cis-1,4 microstructure.

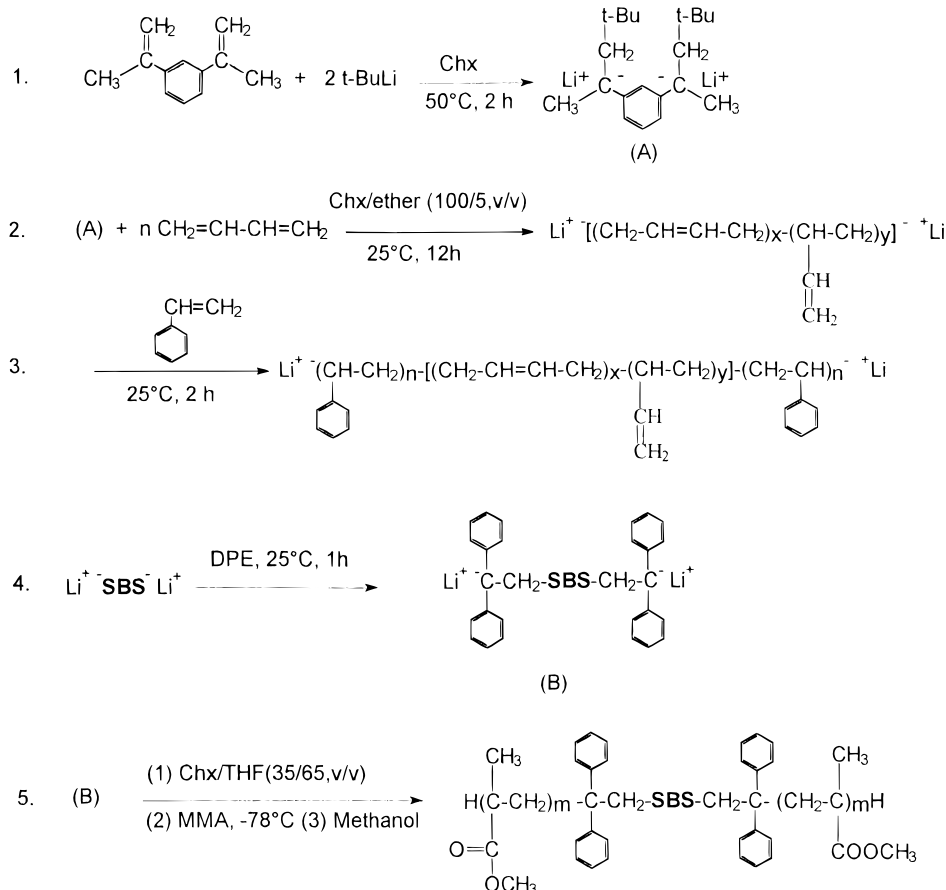
In the previously reported MSBSM pentablocks,¹⁰ PBD was the major component (70 wt %) and contained a low amount of 1,2-units (15%). This paper deals with a simplified synthesis of MSBSM pentablock copolymers that results in PBD midblocks of a higher 1,2-unit content (~43%), which provides the copolymer with improved elastic properties upon hydrogenation.⁴¹ Spe-

* To whom correspondence should be addressed.

[†] Current address: ICI Polyurethanes, Everslaan 45, B-3078 Everberg, Belgium.

[®] Abstract published in *Advance ACS Abstracts*, August 1, 1997.

Scheme 1. Five-Step-Synthesis of MSBSM Pentablock Copolymers



cial attention will be paid to the thermal properties and phase morphology of a series of pentablocks covering a large composition range, i.e., 11–55 wt % PMMA, 18–55 wt % PS, and 15–64 wt % PBD phases. Tensile properties of copolymers of a high PBD content (65 wt %) have also been studied with dependence on the casting solvent.

Experimental Section

Materials. Cyclohexane (Chx) and diethyl ether were dried over CaH_2 for 24 h. THF was purified by refluxing over the deep purple sodium–benzophenone complex. All the solvents were further distilled from polystyryllithium under reduced pressure immediately before use. *tert*-Butyllithium (*t*-BuLi) (Aldrich, 1.3 M solution in cyclohexane) was diluted with cyclohexane, and the final concentration (0.2 N) was determined by double titration.²⁹ *m*-Diisopropenylbenzene (*m*-DIB, Aldrich) was dried over CaH_2 for 24 h and finally distilled from fluorenyllithium before use. 1,1-Diphenylethylene (DPE, Aldrich) was dried over *s*-BuLi and distilled from (diphenylmethyl)lithium before use. Butadiene was dried over *n*-butyllithium. Styrene and methyl methacrylate (MMA) (Aldrich) were distilled from CaH_2 under reduced pressure and stored under nitrogen at -20°C . Before polymerization, MMA was added with a 10 wt % AlEt_3 solution in hexane until a persistent yellowish green color was observed. It was then redistilled under reduced pressure just prior to use. Styrene was redistilled from fluorenyllithium.

Polymerization. Block copolymerization was carried out in a 2-L round-bottomed flask equipped with a magnetic stirrer under a dry nitrogen atmosphere. Details of the experimental techniques and reaction conditions were reported elsewhere.^{9,10} Briefly, the five-step synthesis was as shown in Scheme 1: (1) preparation of the difunctional lithium initiator (DLI) by addition of *t*-BuLi to *m*-DIB (2/1 molar ratio) in cyclohexane at 50°C for 2 h, (2) polymerization of butadiene initiated by DLI in a Chx/diethyl ether (100/5, v/v) mixture at room

temperature for ca. 12 h, (3) polymerization of styrene initiated by the PBD dianions at room temperature for 2 h, (4) end-capping of SBS dianions by diphenylethylene (DPE), and (5) addition of THF to Chx resulting in a Chx/THF (35/65, v/v) mixture followed by the addition of MMA at -78°C . When the butadiene polymerization was complete, an aliquot of the polymer solution was picked out and protonically deactivated. The polymer formed was recovered by precipitation into methanol and used to characterize the PBD block. The same procedure was also used for the characterization of the SBS precursor. Final block copolymers were recovered by precipitation in methanol and dried at room temperature for 2 days under vacuum. The synthesized pentablock copolymers are listed in Table 1.

Isotactic PMMA (*i*PMMA) was prepared in toluene at -78°C with *t*-BuMgBr as initiator according to a method reported by Hatada et al.⁴³ The molecular characteristics were as follows: $M_n = 30\,000$; $M_w/M_n = 1.10$; isotactic triad content = 90%; $T_g = 50^\circ\text{C}$.

Film Preparation. Block copolymers were added with 1 wt % hindered phenol antioxidant (tetrakis[[(methylenedioxy)carbonyl]-3-(3,5-di-*tert*-butyl-4-hydroxyphenyl)propionyl]-methane, Irganox 1010, Ciba-Geigy Corp.) and dissolved in toluene at room temperature. In the case of stereocomplexation, block copolymer and *i*PMMA were separately dissolved in toluene at room temperature. The solutions were then mixed at 100°C , since mixing at room temperature immediately resulted in a gel. This homogeneous solution (8 wt % copolymer) was poured into a Petri dish, and the solvent was allowed to evaporate slowly over 3–4 days at room temperature. Films were dried to constant weight in a vacuum oven at 40°C . They were elastomeric and transparent with a smooth surface.

Analysis. Molecular weight and molecular weight distribution were measured by size exclusion chromatography (SEC) with a Waters GPC 501 apparatus equipped with linear Styragel columns. THF was the eluent (flow rate of 1 mL/min), and polystyrene standards were used for calibration. The

Table 1. Characterization of MSBSM Pentablocks Synthesized with the *m*-DIB/*t*-BuLi Diadduct as Difunctional Initiator

samples	10 ⁻³ <i>M_n</i> ^a M-S-B-S-M	composition (wt %) ^b			microstructure (%) ^b		<i>M_w</i> / <i>M_n</i> ^c
		M	S	B	1,2-(B)	syndio(M)	
P1	4-20-25-20-4	11 (10)	55 (60)	34 (30)	41	80	1.10
P2	6-12-60-12-6	13 (13)	25 (25)	62 (62)	43	80	1.10
P3	9-9-60-9-9	19 (20)	19 (20)	62 (60)	40	80	1.10
P4	19-18-79-18-19	25 (25)	24 (25)	51 (50)	43	80	1.15
P5	17-31-34-31-17	26 (25)	48 (50)	26 (25)	42	80	1.20
P6	23-21-55-21-23	32 (33)	29 (32)	38 (35)	46	80	1.10
P7	23-22-17-22-23	43 (42)	41 (42)	16 (16)	43	80	1.10
P8	31-17-17-17-31	55 (55)	30 (30)	15 (15)	42	80	1.15

^a By SEC with the universal calibration for the B block, by ¹H NMR for the S and M blocks. ^b By ¹H NMR, the theoretical composition is in parentheses. ^c By SEC.

method by Benoit et al.³⁰ for the universal calibration was used with the following viscosimetric relationships:

$$[\eta] = 1.36 \times 10^{-4} M^{0.714} \text{ (PS in THF)}^{31}$$

$$[\eta] = 4.57 \times 10^{-4} M^{0.693} \text{ (PBD in THF)}^{32}$$

¹H NMR spectra were recorded with a Bruker AM-400 spectrometer, by using CDCl₃ as a solvent at 25 °C. The 1,2-unit content of PBD was calculated from the relative intensity of the signal at 4.9 ppm (=CH₂ of 1,2-double bond) and the signal at 5.4 ppm (CH= of 1,2-double bond and -CH=CH- of 1,4 unit). The copolymer composition was calculated from the relative intensity of the signals for the 1,2-unit in PBD, the phenyl ring in PS (6.5 and 7.1 ppm), and the O-CH₃ group in PMMA (3.54 ppm). *M_n* for the PS and PMMA blocks was calculated from the copolymer composition and PBD molecular weight.

Differential scanning calorimetry (DSC) was carried out with a DuPont 900 instrument, calibrated with indium. The usual heating rate was 20 °C/min. The glass transition temperature was noted at the inflection point of the heat capacity jump.

Dynamic mechanical analysis (DMA) was carried out with a TA 983 dynamic mechanical analyzer. Samples (8 × 10 × 0.5 mm) were deformed at a constant 1 Hz frequency.

Toluene-cast films were microtomed into 70 nm thick sections, which were exposed to a 1% aqueous solution of OsO₄ or RuO₄ for 2 h before being observed with a transmission electron microscope (model Philips CM-12) using a 100 kV accelerating voltage.

Tensile measurements were conducted with a Adamek Lhomargy tensile tester. Microdumbbell-shaped testing samples (30 × 3.6 × 1 mm) were cut from toluene-cast films and extended at 200 mm/min at room temperature. The reported data were average values of three independent measurements.

Results and Discussion

Synthesis of Block Copolymers. In a previous paper,¹⁰ we reported the synthesis of MSBSM pentablock copolymers by using a seeding technique for the initiation of the first block. A simplified method has, however, been reported from our laboratory;⁹ i.e., the diadduct of *t*-BuLi onto *m*-DIB prepared in cyclohexane at 50 °C can be directly used to initiate the butadiene polymerization in a cyclohexane/diethyl ether (100/5, v/v) mixture. Under these conditions, well-defined MBM triblock copolymers result from the sequential anionic polymerization of butadiene and methyl methacrylate (MMA). The 1,2-unit content of the PBD block is then relatively high (~40%) due to diethyl ether used in order to promote the formation of triblock copolymers. Nevertheless, this particular microstructure is an efficient means of preventing the midblock from crystallization when hydrogenated with the purpose of increasing the thermooxidation resistance of MBM triblock copolymers.⁴¹ This simplified synthesis technique has been successfully used in this work for preparing

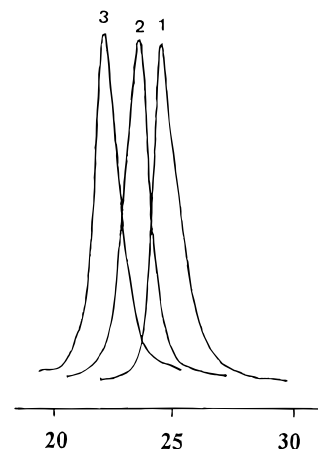


Figure 1. Typical SEC traces for the PBD precursor (trace 1), the SBS intermediate triblock (trace 2), and the MSBSM pentablock copolymer P8 (trace 3) (Table 1).

MSBSM pentablock copolymers, as shown in Scheme 1. It is worth noting that the reaction medium completely gels upon the MMA polymerization. The gel, however, dissolves when the reaction is terminated by addition of a small amount of methanol and warmed to room temperature. The same observation was reported in the case of the synthesis of MBM triblock copolymers. Table 1 shows the molecular weight, molecular weight distribution, and microstructure for the synthesized MSBSM pentablock copolymers. All these samples have a narrow molecular weight distribution (*M_w*/*M_n* < 1.20). Figure 1 shows typical SEC traces monitored after each step of the sequential polymerization of butadiene, styrene, and MMA in the case of the P8 pentablock. The three chromatograms are symmetrical and of a very narrow molecular weight distribution, which indicates that cross-reactions from butadiene anions to styrene and from styrene anions end-capped by DPE to MMA are essentially quantitative. The experimental composition is in good agreement with the theoretical value, as shown in Table 1. The microstructure of the PBD block is systematically in the range 40–46% 1,2-units, as analyzed by ¹H NMR. The PMMA tacticity is also essentially constant with an 80% syndiotactic content.

The polybutadiene (PBD) midblock of the P4 pentablock has also been selectively hydrogenated into a saturated poly(ethylene-*co*-1,2-butene) (PEB) block (sample HP4, Table 3). The quantitative hydrogenation of the PBD midblock has been ascertained by ¹H NMR and FT-IR.⁴¹ The hydrogenated copolymer will be designated as MSEBSM.

SBS and MBM triblock copolymers (Table 2) of a narrow molecular weight distribution have been prepared for the sake of comparison. Their microstructure and molecular weight are comparable to the P4 penta-

Table 2. Characterization of SBS and MBM Triblock Copolymers and MS Diblock Block Copolymers

sample	copolymer	$10^{-3}M_n^a$	composition (wt %) ^b			microstructure(%) ^b		M_w/M_n^c	DSC (°C) ^d		DMA (°C) ^e	
			M	S	B	1,2-(B)	syndio(M)		T_{g1}	T_{g2}	T_{g1}	T_{g2}
T1	S-B-S	20–80–20		33	67	45		1.10	–60	95	–58	100
T2	M-B-M	20–80–20	33		67	45	80	1.10	–60	125	–56	136
D1	M-S	10–10	50	50			80	1.10	110			
D2	M-S	20–20	50	50			80	1.10	107	127		
D3	M-S	40–60	40	60			80	1.10	110	132		

^a By SEC with the universal calibration for the B block, by ¹H NMR for the S and M blocks. ^b By ¹H NMR. ^c By SEC. ^d Heating rate of 20 °C/min. ^e Heating rate of 5 °C/min.

block. Three poly(MMA-*b*-styrene) (MS) copolymers of different molecular weights and compositions have been synthesized as models for the hard blocks in the pentablock copolymers (Table 2). These copolymers have a very narrow molecular weight distribution ($M_w/M_n < 1.10$) and a microstructure comparable to the pentablock copolymers. Glass transition temperatures are also shown in Table 2.

Differential Scanning Calorimetry (DSC). DSC is a very useful technique to detect phase separation in binary blends and block copolymers containing immiscible polymeric components, provided that the individual glass transition temperatures (T_g) are sufficiently different from each other and that the weight composition is far enough from the extreme values. The DSC traces reported for toluene-cast films of the available MSBSM pentablock copolymers are essentially identical in shape and number of prominent features. Typical examples recorded as a result of a second scan at 20 °C/min are shown in Figure 2A for samples P7 (trace 1) and P5 (trace 2). Two main transitions are clearly observed, at ca. –60 °C for both samples and 107 °C for sample P7 and 106 °C for sample P5, respectively. It is known that PBD that contains ca. 45% 1,2-units shows a glass transition at ca. –60 °C (by DSC) in MBM triblock copolymers.⁹ The glass transition temperature for PS ($M_n = 20\,000$) in SBS and PMMA ($M_n = 20\,000$) in MBM is 95 and 125 °C, respectively (Table 2). Thus, the lower temperature transition (–60 °C) in MSBSM pentablock copolymers is characteristic of the PBD phase. The glass transitions for PS and PMMA cannot be distinguished, since a unique T_g is observed at an intermediate value at two different heating rates (Figure 2A, traces 2 and 3). This observation does not result from an inappropriate copolymer composition, since PS and PMMA content in the P7 copolymer is at least 40 wt %. The molecular weight of the PS and the PMMA blocks is also relatively high (>20 000), and high enough to observe two T_g 's in MS diblocks of comparable molecular weights.²⁰ In order to understand better the effect of molecular weight on the phase separation in MS diblock copolymers, three copolymers of different molecular weights have been synthesized and analyzed by DSC (Figure 2B). Sample D1 of lower molecular weight (M-S: 10 000–10 000) shows only one T_g , which suggests phase mixing (trace 1, Figure 2B). In contrast, two T_g 's are observed for the higher molecular weight samples D2 (M-S: 20 000–20 000) and D3 (M-S: 40 000–63 000) (Table 2, Figure 2B), although less clearly in case of sample D2, indicating that phase separation in these MS diblock copolymers is sharp enough to observe two T_g 's provided that the molecular weight is 20 000 and higher for each block. It is worth noting that these results are in good agreement with literature data, since two T_g 's have been reported for an MS diblock copolymer of the same molecular weight (20 000–20 000).²⁰ The reason for a single T_g for the binary hard phase of the pentablock copolymers

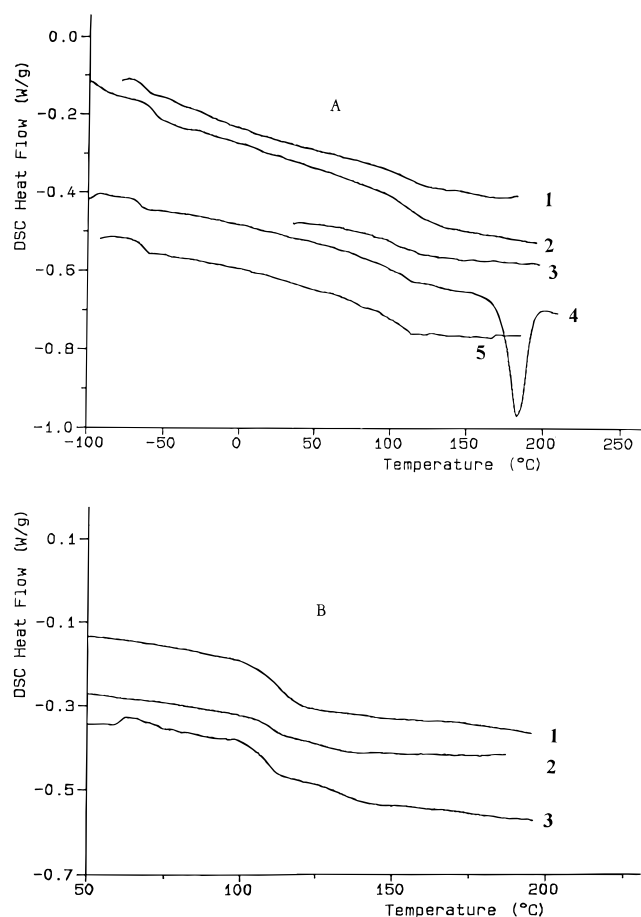


Figure 2. DSC thermograms recorded at a heating rate of 20 °C/min for (A) MSBSM pentablock copolymers (Table 1) [(1) P7, (2) P5, (3) P5 (heating rate: 10 °C/min), (4) CP5 (blend of P5 with iPMMA in a 2/1 s/i mixing ratio), (5) CP5 (second scan)] and (B) M-S diblock copolymers (Table 1) [(1) D1, (2) D2, (3) D3].

would thus be due to the additional PBD midblock, which would prevent PMMA and PS from phase separating. Actually, PBD is highly incompatible with both PS and PMMA in the parent diblocks, whereas PS and PMMA are comparatively less mutually immiscible.²³ In order to minimize the overall interfacial free energy, the system tends to reduce the surface of the PBD domains in favor of the PS and PMMA interface,²³ thus resulting in a PS/PMMA interphase broad enough for the glass transitions of PS and PMMA to be indistinguishable. It is, however, worth noting that three T_g 's were observed for an MSB triblock copolymer containing PS and PMMA blocks of a higher molecular weight (M-S-B: 38 000–116 000–38 000).²⁴

Stereocomplexation of MBM triblock copolymers with iPMMA has been reported to be efficient in extending the service temperature of the original thermoplastic elastomers up to 180 °C.⁴⁴ In order to confirm that stereocomplexation occurs in the hard phase independ-

Table 3. Thermal Properties of MSBSM and MSEBSM Pentablock Copolymers and Blends with *i*PMMA (Heating Rates for DSC and DMA are 20 and 5 °C/min, Respectively)

sample	DSC (°C)				DMA (°C)		
	T_{g1} (°C)	T_{g2} (°C)	T_m (°C)	ΔH (J/g) ^a	T_{g1}	T_{g2}	post T_g
P1	-63	93			-63	105	
P2	-60	114			-55	118	
P3	-58	116			-56	122	
P4	-60	110			-55	130	
HP4	-50	112	7	16	-49	128	
P5	-58	106			-55	133	
CP5	-66	92	182	35	-60	128	>170
P6	-56	107			-54	123	
CP6	-66	115	184	33	-60	120	>170
P7	-62	107			-60	125	
P8	-66	106			-63	123	

^a Melting enthalpy, J/g of EB for sample HP4, J/g of total PMMA for samples CP5 and CP6.

ently of the presence of the PS phase, MSBSM pentablock copolymers P5 and P6 have been blended with isotactic PMMA (*i*PMMA) in a syndio/iso mixing ratio of 2/1, and films have been cast from toluene. These blends are referred to as CP5 and CP6 (Table 3). A typical DSC thermogram is shown in Figure 2A (trace 4) for the CP5 blend. A well-defined endotherm is observed at 185 °C, which corresponds to the stereocomplex of the *s*PMMA end blocks with *i*PMMA. The melting enthalpy of the stereocomplex is quite comparable to the value reported in the case of the MBM/*i*PMMA blends,⁴⁴ suggesting that the PS block does not significantly affect PMMA stereocomplexation. T_{g1} of blends is shifted to lower temperature compared to the parent pentablock copolymer for both CP5 and CP6 (Table 3). Interestingly enough, an additional T_g is observed at 92 °C in the case of CP5, which is quite similar to the T_g of the PS phase and indicates that stereocomplexation of the *s*PMMA end block with *i*PMMA is favorable to the PMMA and PS phase separation. It is worth noting that the stereocomplex melting can only be observed in the first DSC scan, crystallization being prevented from occurring in the bulk (trace 5, Figure 2A).

The HP4 hydrogenated sample shows a broad melting endotherm at 7 °C due to the partial crystallization of the PEB midblock. In parallel, T_g of the soft phase is higher compared to the parent unsaturated copolymer P4.

Dynamic Mechanical Analysis (DMA). The thermal dependence of the dynamic shear storage modulus (G') and the loss factor ($\tan \delta$) has been analyzed for pentablock copolymers of different compositions in the temperature range from -100 to +200 °C at 1 Hz frequency. Figures 3–6 confirm that all these copolymers are phase separated, since two transitions are clearly observed, which are characteristic of the glass transition for the PBD soft phase at the lower temperature (T_{g1}) and for the hard phase at the higher temperature (T_{g2}). In agreement with the DSC analysis, only one transition is observed for the binary MS hard phase in MSBSM pentablock copolymers. The temperature at the maximum of the $\tan \delta$ curves is reported in Table 3.

Figure 3 compares the dynamic mechanical properties of the MSBSM pentablock copolymer P4, the SBS triblock copolymer T1 and the MBM triblock copolymer T2. The molecular weight of the PS block (18 000) and the PMMA block (19 000) in sample P4 is quite com-

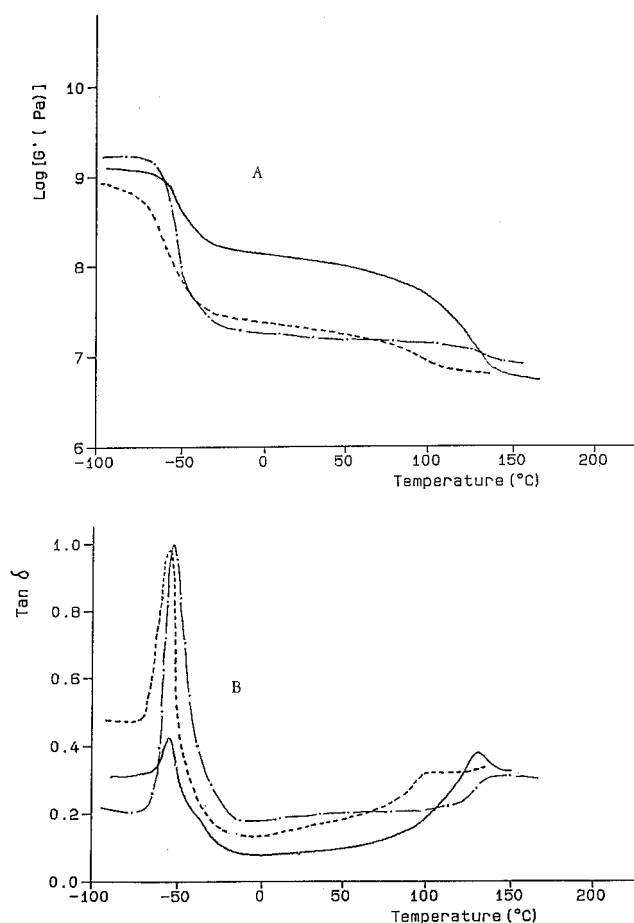


Figure 3. Temperature dependence of shear storage modulus (G') (a) and loss $\tan \delta (=G''/G')$ (b) at 1 Hz and a heating rate of 5 °C/min for the SBS sample T1 (---), MBM sample T2 (-·-), and MSBSM sample P4 (—).

parable to the end blocks in the SBS and MBM triblock copolymers, respectively (Table 2). Figure 3 shows that the storage modulus (G') in the rubbery plateau is quite comparable for the SBS and MBM samples of comparable hard block content, indicating that the nature of the outer block does not significantly affect G' in this region. A significant difference is, however, observed at temperatures higher than 80 °C, beyond which G' of SBS rapidly decreases in contrast to G' of MBM, which persists up to 130 °C. G' for the rubbery pentablock P4 is much higher than for the parent SBS and MBM copolymers as a result of a 2-fold higher hard block content. The transition from the rubbery plateau to the viscous flow for P4 occurs at a temperature intermediate between the temperatures reported for the SBS and MBM copolymers, respectively. In parallel, although the loss peak characteristic of the soft phase is essentially the same for the three samples, the situation is different for the loss peak of the hard phase. The loss peak for the PS end blocks of SBS is observed at 100 °C, compared to 136 °C for the PMMA end blocks of MBM, whereas a unique but broader loss peak is reported for the binary hard phase of the pentablock P4 at 130 °C, thus at an intermediate temperature with respect to the SBS and MBM counterparts, indicating an at least partial phase mixing of the PS and PMMA blocks in P4.

Figure 4 illustrates the dynamic mechanical properties for the P2 and P3 samples, which have the same hard phase content but a different PMMA/PS wt ratio. The thermal dependence of G' is quite comparable for

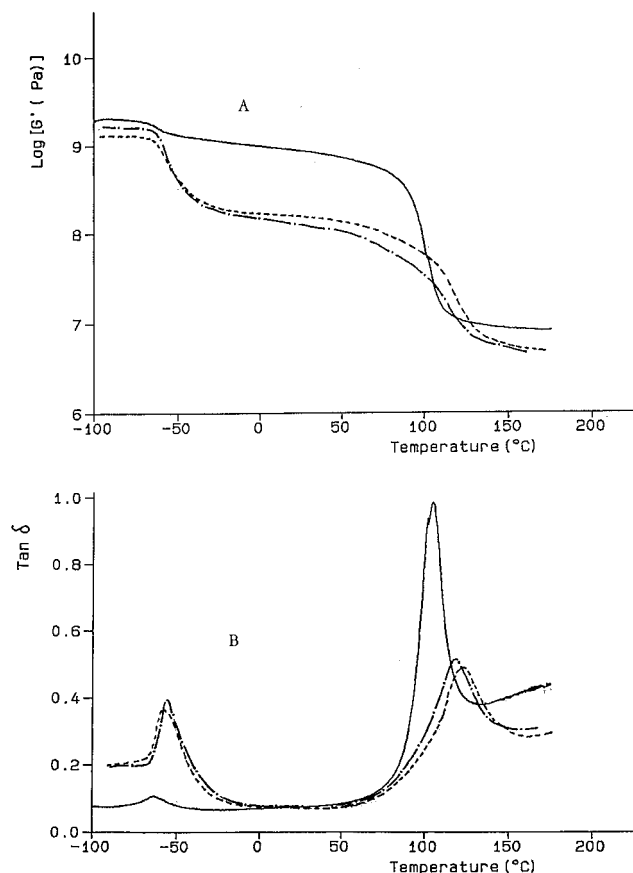


Figure 4. Temperature dependence of shear storage modulus (G') (a) and loss $\tan \delta (=G''/G')$ (b) at 1 Hz and a heating rate of 5 °C/min for the MSBSM samples P1 (—), P2 (---), and P3 (- - -).

these samples in the T_g region (Figure 4), whereas G' at higher temperatures is smaller for sample P2 which is of a lower PMMA content compared to P3. Consistently, the loss peak for the hard phase of sample P3 is observed at a slightly higher temperature than for P2 (Figure 4). The effect of the relative content of PMMA in the hard phase on the transition temperature of that phase is more pronounced when samples P1 and P2 are compared. The hard phase of sample P1 contains 17 wt % PMMA, i.e., half the content calculated for sample P2 (33 wt %), although the molecular weight of the PMMA block is essentially the same (Table 1). Clearly, T_g for the hard phase of P2, which contains more PMMA, is significantly higher compared to P1 (Figure 4 and Table 3). The much higher hard phase content of P1 accounts for a substantially higher G' in the rubbery plateau compared to P2 and P3.

T_g for the PBD phase (T_{g1}) measured by DMA is smaller for the MSBSM copolymers P1, P7, and P8 compared to the other samples (Table 3), as a possible result of the comparatively lower molecular weight of the PBD block.

In order to confirm that the observation of a single T_g for the hard phase of the MSBSM copolymers P1–P4 is not due to a too low hard phase content (<66 wt %), sample P7 of a high hard phase content (84 wt %) has been analyzed. Figure 5 shows the dynamic mechanical curves above 0 °C. Only one T_g is observed at two different heating rates (5 and 1 °C/min).

According to DSC, T_g of the PS phase can be observed when pentablocks are mixed with *i*PMMA. It is the reason why CP5 and CP6 blends have also been analyzed by DMA, as shown in Figure 6 for the CP5

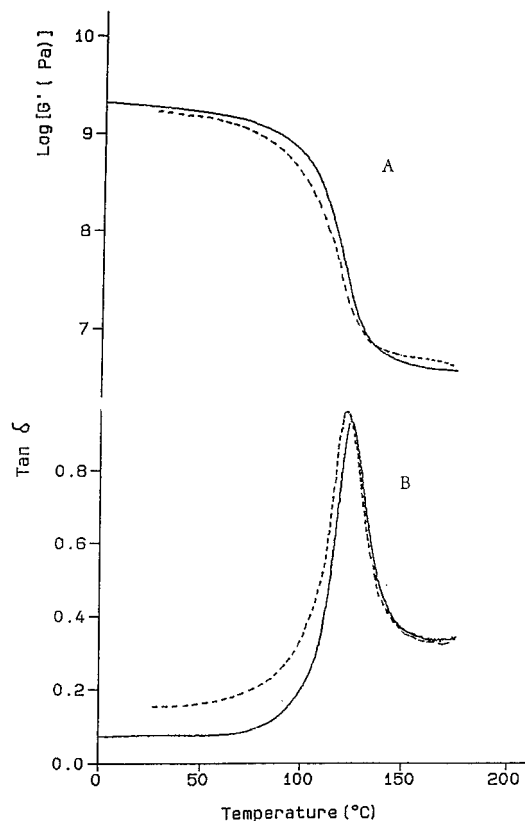


Figure 5. Temperature dependence of shear storage modulus (G') (a) and loss $\tan \delta (=G''/G')$ (b) at 1 Hz for the MSBSM samples P7 with a heating rate of 5 °C/min (—) and 1 °C/min (---).

blend and the parent pentablock copolymer P5. G' in the rubbery plateau is higher for the CP5 blend compared to the pentablock P5 (Figure 6) as result of a higher hard phase content. The glass transition temperature of the PBD soft phase is shifted to lower temperature when P5 is mixed with *i*PMMA, in agreement with DSC. The lower PBD content of CP5 compared to P5 accounts for the smaller damping at the T_g of the soft phase. Two transitions seem to be observed for sample CP5 in the glass transition region for the hard phase. A $\tan \delta$ maximum is observed at a slightly lower temperature and with a smaller damping compared to the parent copolymer. This transition is quite broad, indicating a broad distribution of relaxation times, which might result from the overlapping of the relaxation of the PS and noncomplexed PMMA. The PMMA stereocomplex, whose melting is observed at 182 °C by DSC, starts to relax in this temperature range (in which the accuracy of the experimental measurements decreases). When a second scan is carried out after the complete melting of the stereocomplex (Figure 6), no change is observed for the glass transition of the soft phase, in contrast to the relaxation of the hard phase, which occurs at a temperature lower than that for the parent copolymer P5 due to the presence of *i*PMMA of a lower T_g (50 °C). This additional compound in the hard phase explains why the amplitude of the damping has increased (compared to P5).

Morphological Observations. The equilibrium phase morphology of binary block copolymers is known to be dictated by their composition, as previously reported for SB, SBS, and MBM triblock copolymers.^{9,11,33} Lamellae, hexagonally packed cylinders, and body-centered cubic arrays of spheres are the three classical morphologies displayed by the binary block

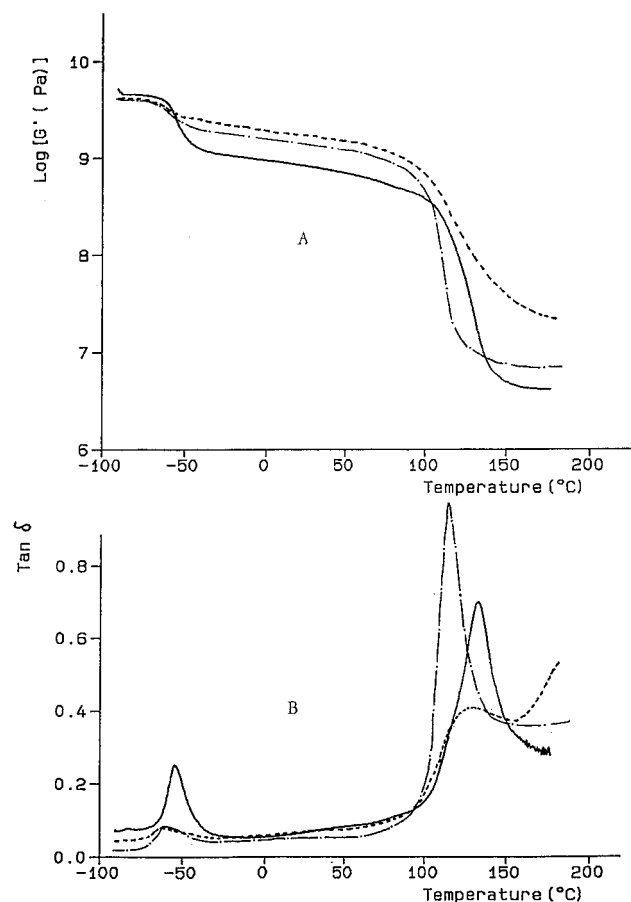


Figure 6. Temperature dependence of shear storage modulus (G') (a) and loss $\tan \delta (=G''/G')$ (b) at 1 Hz and a heating rate of 5 °C/min for the MSBSM sample P5 (—) and its blend with iPMMA in a 2/1 s/i mixing ratio, first scan (---) and second scan (-.-).

copolymers. As a rule, a spherical morphology is observed for a PBD content in the 0–18 wt % range. When the PBD content is as high as 18–38 wt %, a cylindrical morphology is usually observed, whereas a lamellar morphology is reported for 36–60 wt % PBD.¹¹ Recently, some nonclassical morphologies have been reported. The first one, observed in 1976¹² and identified in 1986,¹³ is the ordered bicontinuous double-diamond (OBDD). The second one is the bicontinuous gyroid phase reported by Hajduk et al. for a poly(styrene-*b*-isoprene) (SI) diblock.¹⁵ Another nonclassical morphology is the catenoid–lamellae,^{14,16,34} in which each lamella is covered by hexagonally arranged cylinders. “Mesh” and “strut” structures have also been reported by Hashimoto et al. for SB star-block/homoPS mixtures.^{36,37}

These morphologies have essentially been reported for binary systems. In contrast to binary block copolymers, whose composition is the main parameter that determines the equilibrium microphase structure, the morphology of ternary block copolymers is dictated not only by two independent composition variables but also by the balance of the three interaction parameters and the respective interfacial tensions.²⁴ Mogi et al.^{18,19} have studied a series of poly(isoprene-*b*-styrene-*b*-2-vinylpyridine) (ISP) triblock copolymers and observed a highly ordered tricontinuous double-diamond morphology as well as a morphology in which the PIP and PVP domains form cylinders in a PS matrix. A chiral supramolecular assembly has been reported by Stadler et al. for poly(styrene-*b*-butadiene-*b*-methyl methacry-

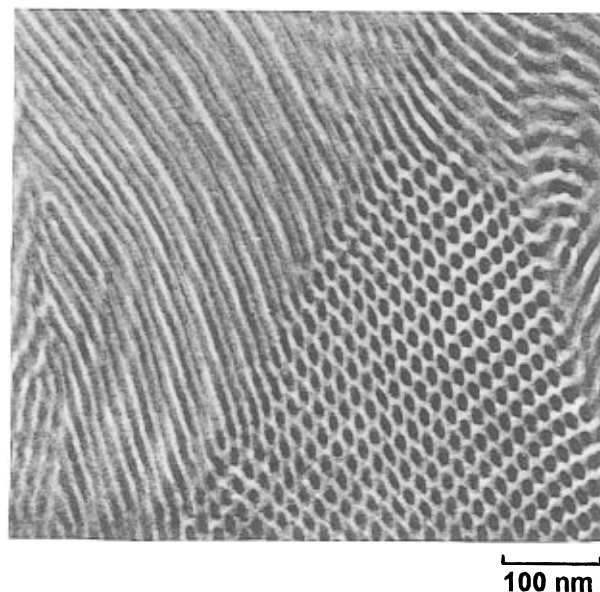


Figure 7. Transmission electron micrograph for the MSBSM pentablock copolymer P1. PBD is the black phase stained with OsO₄.

late) (SBM) triblocks in which the polybutadiene mid-block forms helical strands surrounding polystyrene cylinders embedded in a poly(methyl methacrylate) (PMMA) matrix.²²

The phase morphology of the ternary MSBSM pentablocks has been analyzed by transmission electron microscopy (TEM), which confirms the phase separation observed by DSC and DMA. Figures 7–10 show transmission electron micrographs of toluene-cast films of copolymers of various compositions annealed at 140 °C for 4 days under vacuum. PBD is observed as the dark phase as result of the selective staining by OsO₄. Figure 7 shows the phase morphology for the copolymer P1 (Table 1), in which PS is the major component, and only a small amount of PMMA is present (11 wt %). A classical cylindrical morphology is observed with PBD cylinders of ca. 12 nm diameter embedded in the hard phase matrix.

PBD is the major component (62 wt %) in samples P2 and P3 (Table 1), so that a cylindrical morphology is expected to be observed. The phase morphology of sample P3 (Figure 8A) is, however, more complex. A lamellar structure is indeed observed with lamellae of a modulated thickness. Actually, this structure resembles the lamellar–catenoid morphology first identified by Thomas et al.³⁴ for a partially annealed solution-cast SB diblock copolymer. These experimental observations are in contrast to the recent theoretical calculation by Fredrickson⁴⁰ suggesting that this morphology is metastable in the strong segregation limit of AB diblock copolymers and to the prediction by de la Cruz et al.¹⁷ that this morphology can only be observed near the order–disorder transition (ODT). It has also been observed for poly(styrene-*b*-isoprene) (SI)/homoPS blends¹⁶ and for poly(ethyl methacrylate) (PEMA)–PBD–PEMA triblock copolymers³⁹ under near-equilibrium conditions. Figure 8B shows the morphology of sample P2. Ellipsoid-like spots (white) hexagonally arranged are observed in addition to the modulated lamellae. This structure is similar to a type of morphology observed for an asymmetrical poly(ethylenepropylene-*b*-ethylene) diblock copolymer near the order–disorder transition by Hamley et al.³⁵ and designated as a layered hexagonal packed channel.

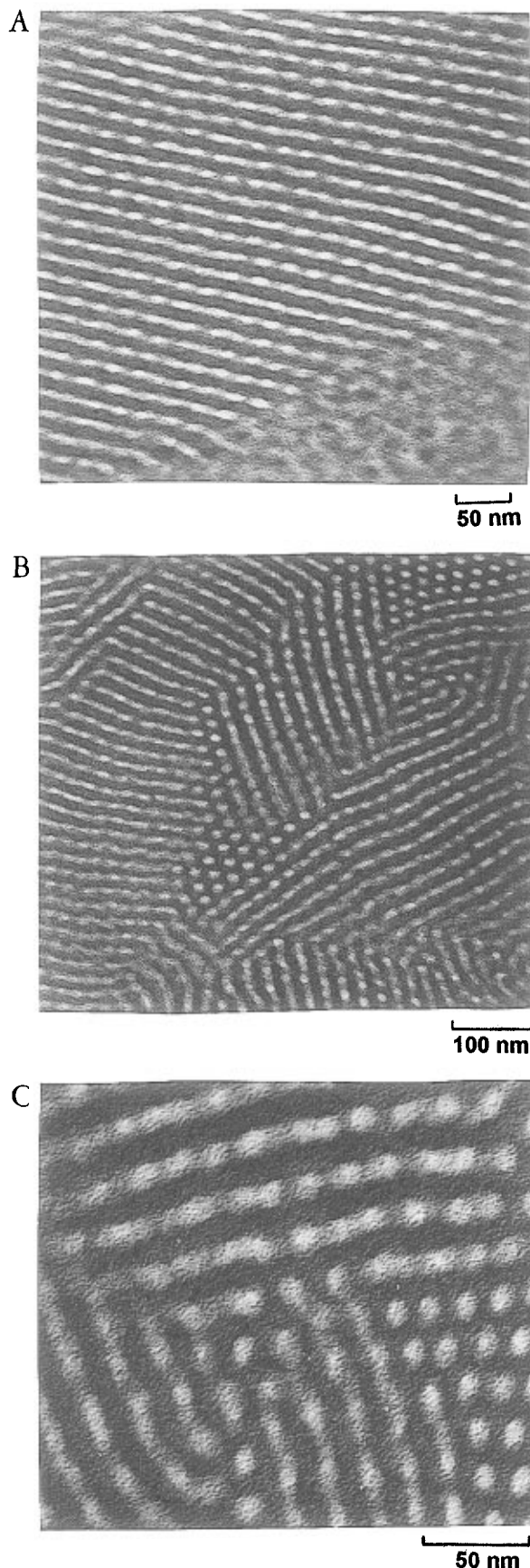


Figure 8. Transmission electron micrographs for the MSBSM pentablock copolymers P3 (A) and P2 at two magnifications (B and C). PBD is the black phase stained with OsO_4 .

Sample P4 contains comparable amounts of hard and soft blocks and shows a morphology consisting of hard

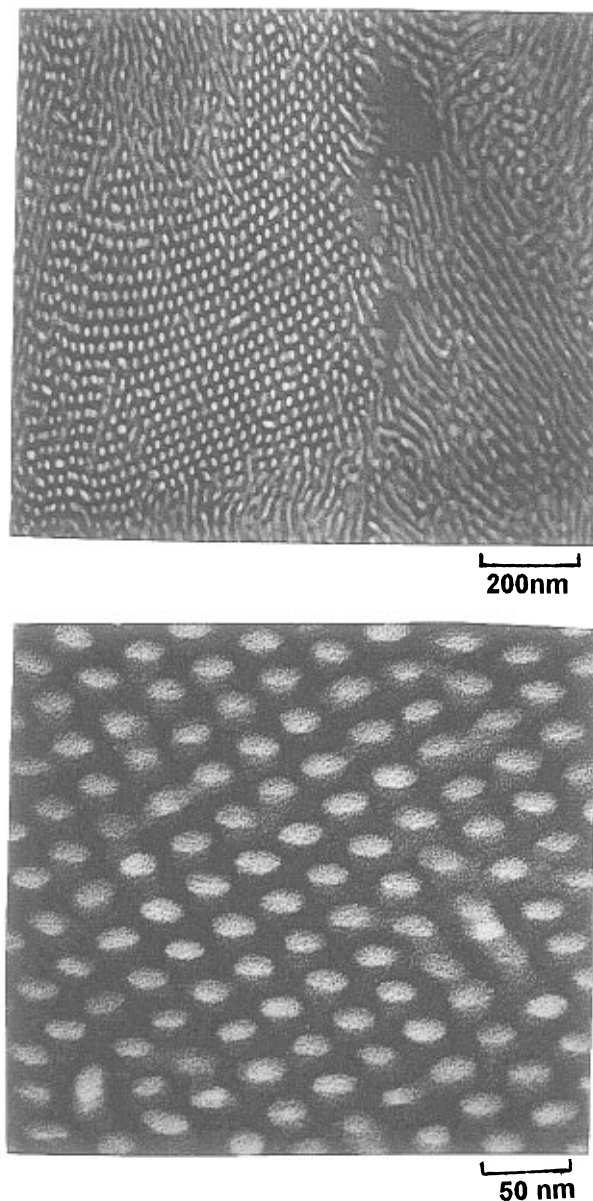


Figure 9. Transmission electron micrographs for the MSBSM pentablock copolymer P4 at two magnifications. PBD is the black phase stained with OsO_4 .

phase cylinders embedded in the PBD matrix (Figure 9).

The micrographs for samples P5 and P6 are shown in Figure 10A,B. A lamellar structure with PBD layers ca. 12 nm thick is observed for sample P6, which contains comparable amounts of the three constitutive components (Figure 10B). Although the PBD content of sample P5 is much smaller than that in sample P6 (38 wt %), lamellar morphology persists (Figure 10A), with comparatively much thinner (ca. 11 nm) PBD layers compared to the thickness of the hard phase (17 nm).

The morphology of sample P7 (16 wt % PBD) is shown in Figure 10C. The dark PBD microphases appear to form ill-shaped lamellae or cylinders connected to each other in a percolation network in a continuous PS/PMMA hard phase, so that the phase morphology fits a bicontinuous network structure. The PBD and the hard phases seem to be uniform. This morphology is quite similar to the "strut" structure reported by Hashimoto et al. for a blend of an SB star block with homoPS.²² The weight ratio of the hard and soft phases in sample

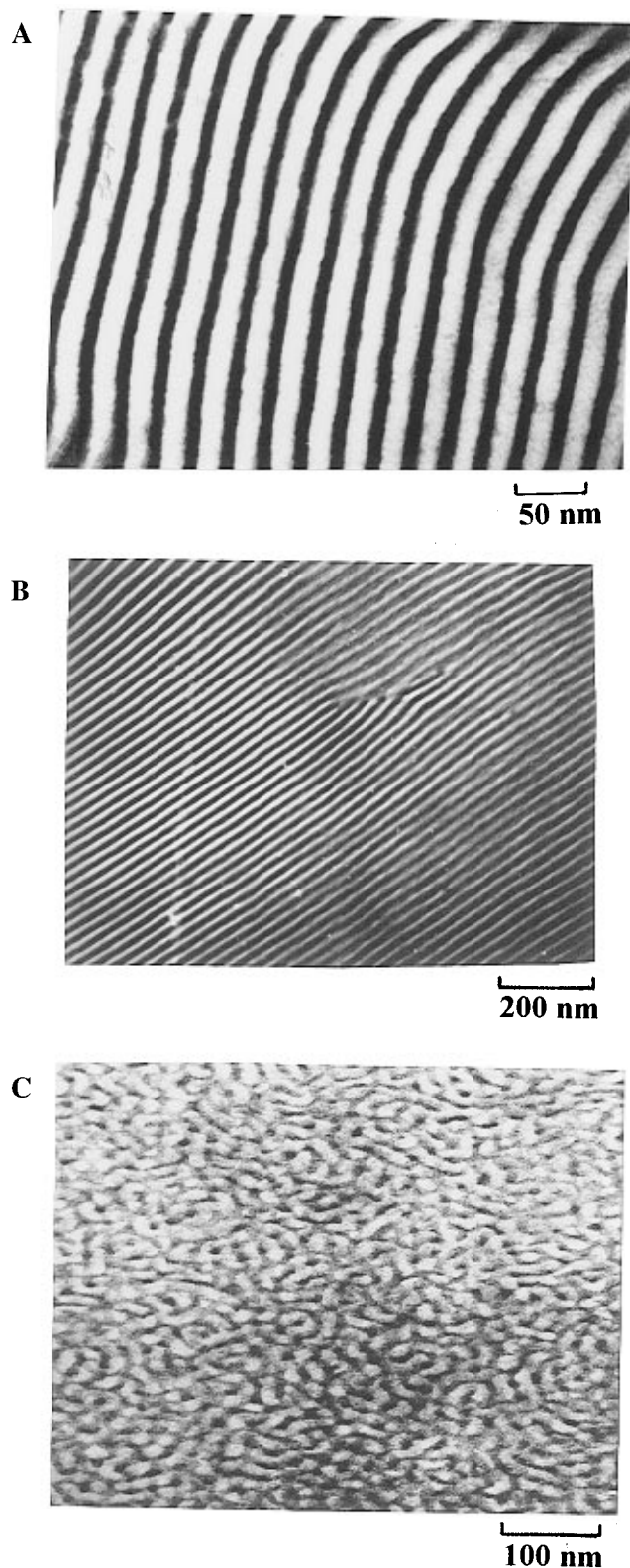


Figure 10. Transmission electron micrographs for the MSBSM pentablock P5 (A), P6 (B), and P7 (C). PBD is the black phase stained with OsO_4 .

P7 (84/16) is very similar to the weight composition of the SB block/PS blend (86/14). The strut morphology is thought to be a new type of cocontinuous structure with less order than the OBDD. A hyperbolic interface with a negative Gaussian curvature is considered as a basic shape of the interface between the links.²²

The electron micrograph of copolymer HP4, which is the hydrogenated version of sample P4, i.e., MSEBSM,

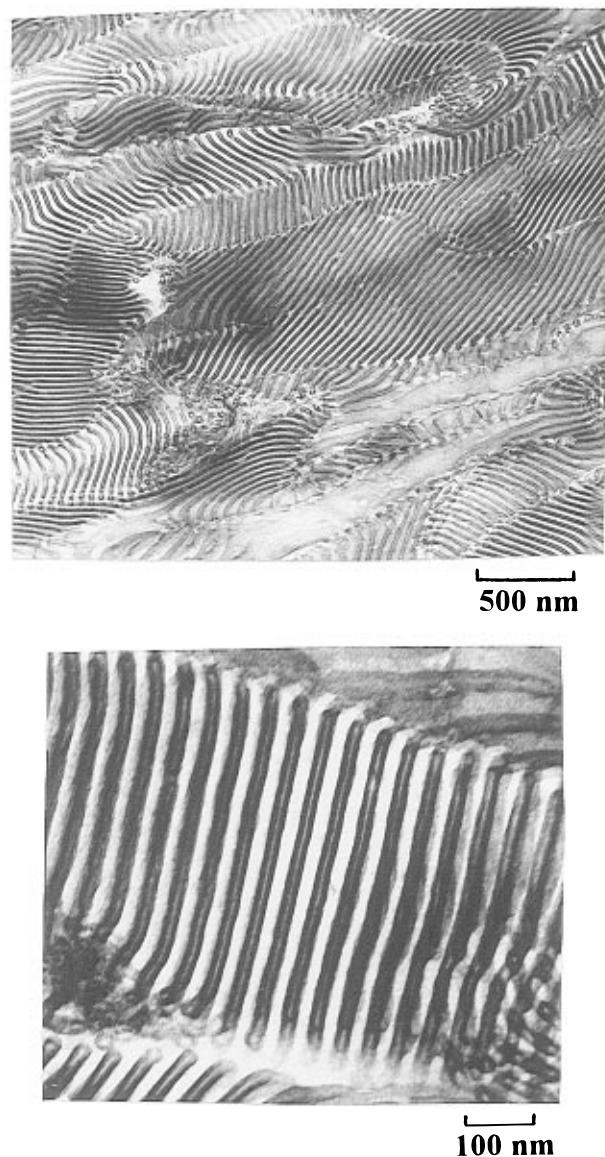


Figure 11. Transmission electron micrographs for the MSEBSM pentablock copolymer HP4 at two magnifications. PS is the black phase stained with RuO_4 .

is shown in Figure 11. This sample was stained with RuO_4 , which selectively stains the PS phase and makes it appear as a dark phase. In contrast to the unsaturated parent copolymer for which a cylindrical morphology was observed (Figure 9), the overall morphology is now a typical lamellar structure of the ABCB type with a long period for the M-S-EB-S repeat unit of ca. 40 nm. The white EB layers are thick compared to the white PMMA layers, which are very thin and sandwiched between the dark PS layers.

It is worth noting that all the samples were prepared by solvent-casting, so that specific solvent effects can play a morphological role in view of the variable composition of the mixture during solvent removal. Annealed samples are thus needed for equilibrium morphological evaluation, which will be the topic of a forthcoming work.

Stress-Strain Behavior. Tensile properties are one of the most interesting features of thermoplastic elastomers. Attention has been paid to the stress-strain behavior of the P2 and P3 pentablock copolymers of a relatively low hard block content. Solvent-cast films have been studied, since this technique has been

Table 4. Mechanical Properties of MSBSM Pentablock Copolymers Cast from Different Solvents

sample	casting solvent	yield stress (MPa)	ultimate tensile strength (MPa)	elongation at break (%)	permanent set at break (%)
P2	toluene	3.5	32.0	900	75
P2	Chx/THF	4.0	28.5	900	75
P2	MEK/THF	5.3	25.3	900	90
P3	toluene	4.8	35.5	850	75
P3	Chx/THF	8.2	31.0	880	75
P3	MEK/THF	6.7	28.0	850	80

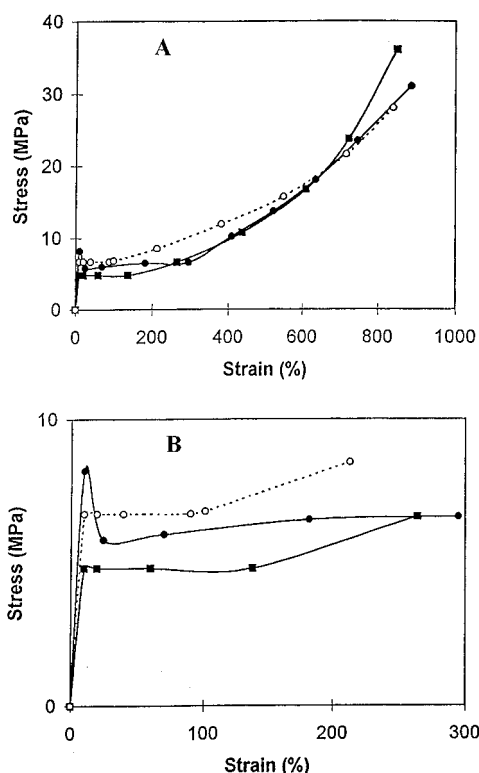


Figure 12. Stress-strain curves for the MSBSM pentablock copolymer P3 cast from different solvents: (A) full curves; (B) curves in the small strain region. Key: (■) toluene; (●) cyclohexane/THF mixture (50/50, v/v); (○) MEK/THF mixture (50/50, v/v)

reported to yield reproducible phase morphology for SBS block copolymers provided the solvent evaporation is slow.³⁸ Morphology and bulk properties of a solvent-cast film, however, depend on the casting conditions, and particularly on the casting solvent.^{9,11,38} Three solvents have been used in this study, i.e., toluene, a 50/50 (v/v) cyclohexane/THF mixture, and a 50/50 (v/v) methyl ethyl ketone/THF mixture. Toluene is a common solvent for PBD, PS, and sPMMA blocks. Cyclohexane (Chx) is a selective solvent for PBD, and methyl ethyl ketone (MEK) selectively dissolves PMMA and PS. Since the MSBSM copolymer is insoluble in cyclohexane and MEK, a mixture of each of these solvents with THF has been used for the sample preparation. Yield stress (σ_y), ultimate tensile strength (σ_b), elongation at break (ϵ_b), and permanent set at break, which is a measurement of the irreversible deformation, are reported in Table 4. Figure 12 shows the typical stress-strain curves for sample P3 measured at room temperature and at a strain rate of 200 mm/min. The tensile stress is expressed as a nominal stress, i.e., the ratio of the tensile force to the original cross-sectional area of the specimen. For the sake of clarity, the stress-strain curves in the small strain region have been expanded in Figure 12B. A yield point at ca. 8% strain is observed whatever the casting solvent, which is indicative of the formation of a semicontinuous hard phase, in agreement

with the catenoid-lamellar morphology observed by TEM (Figure 8A) for the toluene-cast film. This continuous hard phase might be composed of the PMMA and PS phases which are mixed intimately enough to show one T_g by DSC. Beyond the yield point, cold drawing is observed with a well-pronounced intermediate necking for the sample cast from the Chx/THF mixture (Figure 12B). In this case, the stress starts to increase with elongation beyond an elongation of ca. 300%. This increase is observed for a strain of ca. 100% and 150% for samples cast from the MEK/THF mixture and toluene, respectively. The fracture is observed at approximately the same elongation (850%). This behavior is a typical strain-induced plastic-to-rubber transition, or strain-softening behavior, which has also been reported for SBS triblock copolymers.⁴²

The permanent set at break does not significantly depend on the casting solvent. The ultimate tensile strength is higher for toluene-cast films and lower for MEK/THF-cast films, for both P2 and P3 samples. This solvent effect has also been observed for MBM triblock copolymers.⁹ The elongation and the permanent set at break seem to be not significantly affected by the casting solvent. The yield stress not only depends on the casting solvent but also on the composition of samples P2 and P3, since a higher stress is observed for the MEK/THF-cast P2 sample (5.3 MPa) compared to 8.2 MPa for the Chx/THF-cast P3 specimen.

Conclusions

A series of poly[methyl methacrylate (M)-*b*-styrene (S)-*b*-butadiene (B)-*b*-S-*b*-M], or MSBSM, pentablock copolymers have been successfully synthesized with a monomodal and narrow molecular weight distribution (<1.20), in a composition range of 11–55 wt % for the M block, 19–55 wt % for the S block, and 15–62 wt % for the B block.

Toluene-cast films are phase separated, as confirmed by DSC and dynamic mechanical analysis (DMA). While the phase separation of the PBD soft phase is clearly observed, DSC and DMA are unable to distinguish PS and PMMA phases.

Classical morphologies, such as cylindrical and lamellar structures, have been observed by transmission electron microscopy (TEM) for some pentablock copolymers depending on their composition. Two less traditional morphologies, i.e., catenoid-lamellar and strut structures, have also been observed. The phase morphology strongly depends on the chemical structure of the pentablock, since the cylindrical morphology observed for a MSBSM copolymer containing equal amounts of hard and soft phases is changed into an alternative lamellar structure upon hydrogenation of the PBD midblock.

Copolymers of a relatively low hard phase content show the typical behavior of thermoplastic elastomers with high ultimate tensile strength (ca. 30 MPa) and elongation at break (ca. 850%). These mechanical properties are dependent on the casting solvent.

Acknowledgment. The authors are very much indebted to the IWT (Flemish Institute for the Promotion of Science-Technological Research in Industry) for the financial support of a joint research program with Raychem N.V. (Kessel-Lo, Belgium) and the Katholieke Universiteit Leuven (Prof. H. Berghmans and H. Reynaers). They warmly thank Dr. N. Overbergh (Raychem, Kessel-Lo), Dr. Ph. Hammond, and Dr. J. Hudson (Raychem, Swindon) for stimulating discussions. They are grateful to the "Services Fédéraux des Affaires Scientifiques, Techniques et Culturelles" for general support in the frame of the "Pôles d'Attraction Interuniversitaires: Polymères". Ph.D. is a Research Associate of the Belgian National Fund for Scientific Research (FNRS).

References and Notes

- (1) Weiss, R. A.; Sen, A.; Pottick, L. A.; Willis, C. L. *Polym. Commun.* **1990**, *31*, 220.
- (2) Weiss, R. A.; Sen, A.; Willis, C. L.; Pottick, L. A. *Polymer* **1991**, *32* (10), 1867.
- (3) Fetters, L. J.; Morton, M. *Macromolecules* **1969**, *2* (5), 453.
- (4) Morton, M.; Mikesell, S. L. *J. Macromol. Sci.-Chem.* **1993**, *A7* (7), 1391.
- (5) Ladd, B. J.; Hogen-Esch, T. E. *Polym. Prepr. (Am. Chem. Soc., Div. Polym. Chem.)* **1989**, *30* (11), 261.
- (6) Long, T. E.; Broske, A. D.; Bradley, D. J.; McGrath, J. E. *J. Polym. Sci., Polym. Chem. Ed.* **1989**, *27*, 4001.
- (7) DePorter, C. D.; Ferrence, G. M.; McGrath, J. E. *Polym. Prepr. (Am. Chem. Soc., Div. Polym. Chem.)* **1993**, *34* (2), 574.
- (8) Quirk, R. P. *Polym. Prepr. (Am. Chem. Soc., Div. Polym. Chem.)* **1985**, *26* (2), 14.
- (9) Yu, J. M.; Dubois, Ph.; Teyssié, Ph.; Jérôme, R. *Macromolecules* **1996**, *29*, 6090.
- (10) Yu, Y.; Dubois, Ph.; Teyssié, Ph.; Jérôme, R. *J. Polym. Sci., Polym. Chem. Ed.* **1996**, *34*, 2221.
- (11) Gallot, B. R. M. *Adv. Polym. Sci.* **1978**, *29*, 85.
- (12) Aggarwal, S. L. *Polymer* **1976**, *17*, 938.
- (13) Thomas, E. L.; Alward, D. B.; Kinning, D. J.; Martin, D. C.; Handlin, D. L.; Fetters, L. J. *Macromolecules* **1986**, *19*, 2197.
- (14) Forster, S.; Khandpur, A. K.; Zhao, J.; Bates, F.; Hamley, I. W.; Ryan, A. J.; Bras, W. *Macromolecules* **1994**, *27*, 6922.
- (15) Hajduk, D. A.; Harper, P. E.; Gruner, S. M.; Honeker, C. C.; Kim, G.; Thomas, E. L.; Fetters, L. J. *Macromolecules* **1994**, *27*, 4063.
- (16) Spontak, R. J.; Smith, S. D.; Ashraf, A. *Macromolecules* **1993**, *26*, 956.
- (17) de la Cruz, M.; Mayes, A. M.; Swif, B. W. *Macromolecules* **1992**, *25*, 944.
- (18) Mogi, Y.; Kotsuji, H.; Kaneko, Y.; Mori, K.; Matsushita, Y.; Noda, I. *Macromolecules* **1992**, *25*, 5408.
- (19) Mogi, Y.; Mori, K.; Matsushita, Y.; Noda, I. *Macromolecules* **1992**, *25*, 5412.
- (20) Sohn, J.; Ree, T. *J. Appl. Polym. Sci.* **1984**, *29*, 4237.
- (21) Auschra, C.; Stadler, R. *Macromolecules* **1993**, *26*, 2171.
- (22) Krappe, U.; Stadler, R.; Voigt-Martin, I. *Macromolecules* **1995**, *28*, 4558.
- (23) Stadler, R.; Auschra, C.; Beckmann, J.; Krappe, U.; Voigt-Martin, I.; Leibler, L. *Macromolecules* **1995**, *28*, 3080.
- (24) Jung, K.; Abetz, V.; Stadler, R. *Macromolecules* **1996**, *29*, 1076.
- (25) Funabashi, H.; Miyamoto, Y.; Isono, Y.; Fujimoto, T.; Matsushita, Y.; Nagasawa, M. *Macromolecules* **1983**, *16*, 1.
- (26) Isono, Y.; Tanisugi, H.; Endo, K.; Fujimoto, T.; Hasegawa, H.; Hashimoto, T.; Kawai, H. *Macromolecules* **1983**, *16*, 5.
- (27) Jérôme, R.; Forte, R.; Varshney, S. K.; Fayt, R.; Teyssié, Ph. In *Recent Advances in Mechanistic and Synthetic Aspects of Polymerization*; Fontanille, M.; Guyot, A., Eds.; NATO ASI series, 215; Kluwer: Dordrecht, The Netherlands, 1987; p 101.
- (28) Varshney, S. K.; Hautekeer, J. P.; Fayt, R.; Jérôme, R.; Teyssié, Ph. *Macromolecules* **1990**, *23*, 2681.
- (29) Gilman, H.; Cartledge, F. K. *J. Organomet. Chem.* **1964**, *2*, 447.
- (30) Benoit, H.; Grubisic, Z.; Rempp, P.; Decker, P.; Zilliox, J. *J. Chim. Phys.* **1966**, *63*, 1507.
- (31) Appelt, B.; Meyerhoff, G. *Macromolecules* **1980**, *13*, 657.
- (32) Yau, W. W.; Kirkland, J. J.; Bly, D. D. *Modern Size Exclusion Liquid Chromatography*; Wiley Interscience: New York, 1979.
- (33) Holden, G.; Legge, N. R. In *Thermoplastic Elastomers*; Legge, N. R., Holden, G., Schroeder, H. E., Eds.; Hanser: Munich, Vienna, New York, 1987; p 47.
- (34) Thomas, E. L.; Anderson, D. M.; Henkee, C. S.; Hoffman, D. *Nature* **1988**, *334*, 598.
- (35) Hamley, I. W.; Koppi, K. A.; Rosedale, J. H.; Bates, F. S.; Almdal, K.; Mortensen, K. *Macromolecules* **1993**, *26*, 5959.
- (36) Hashimoto, T.; Koizumi, S.; Hasegawa, H.; Izumitani, T.; Hyde, S. T. *Macromolecules* **1992**, *25*, 1433.
- (37) Hasegawa, H.; Hashimoto, T.; Hyde, S. T. *Polymer* **1996**, *37*, 3825.
- (38) Beecher, J. F.; Marker, L.; Bradford, R. D.; Aggarwal, S. L. *J. Polym. Sci.* **1969**, *C26*, 117.
- (39) Yu, J. M.; Dubois, Ph.; Teyssié, Ph.; Jérôme, R. *Macromolecules* **1996**, *29*, 8362.
- (40) Fredrickson, G. H. *Macromolecules* **1991**, *24*, 3456.
- (41) Yu, J. M.; Yu, Y.; Dubois, Ph.; Teyssié, Ph.; Jérôme, R. *Polymer* **1997**, *38*, 3091.
- (42) Hashimoto, T.; Fujimura, M.; Saijo, K.; Kawai, H.; Diamant, J.; Shen, M. *Multiphase Polymers*; Advances in Chemistry Series; American Chemical Society: Washington, DC, 1979; No. 176, p 257.
- (43) Hatada, K.; Ute, K.; Tanaka, K.; Kitayama, T.; Okamoto, Y. *Polym. J.* **1985**, *17* (8), 977.
- (44) Yu, J. M.; Yu, Y.; Dubois, Ph.; Teyssié, Ph.; Jérôme, R. *Polymer* **1997**, *38*, 2143.

MA961872H